www.ietdl.org

Published in IET Image Processing
Received on 3rd June 2012
Revised on 13th October 2013
Accepted on 18th October 2013
doi: 10.1049/iet-ipr.2013.0006

ISSN 1751-9659

Different lighting processing and feature extraction methods for efficient face recognition

Jiuzhen Liang, Mei Wang, Zhilei Chai, Qin Wu

Department of Computer Science, Jiangnan University, Wuxi, Jiangsu 214122, People's Republic of China
E-mail: jzliang@jiangnan.edu.cn

Abstract: This study studies different lighting processing and feature extraction methods for efficient face recognition. The purpose is to find some robust face recognition methods by combining different feature extraction methods with illumination compensation. In this study, some typical illumination preprocessing approaches are reviewed including wavelet transformation, self-quotient image, Retinex, smoothing, discrete cosine transform normalisation in logarithm domain, homomorphic filter and local contrast enhancement. As the main contribution, this study proposes two efficient feature extraction methods for face recognition. One is an adaptive feature extraction (AFE) based on curvelet transform. The other is a feature extraction technique named two-dimensional principal component analysis (2DPCA) non-parametric analysis of 2D subspace (2DPCA + 2DNSA). Two groups of experiments are designed to verify the proposed methods. The first group of experimental results show that the proposed AFE methods have better performance than conventional methods. In the second group of experiments, each feature extraction method is combined with nine different lighting processing methods. The results show that the proposed 2DPCA + 2DNSA method is more robust to lighting processing than other methods. Experimental results also show that lighting processing contribution to face recognition are quite different for different face databases.

1 Introduction

Face recognition is a challenging research topic [1]. Even for the same person, the same face appears differently because of lighting conditions, expression, pose, occlusion and other confounding factors in real life [2]. Among all of them, illumination is the most significant factor that alters the perception or appearance of faces [3]. The variation between images of the same face because of illumination and viewing direction is almost always larger than image variations because of change in face identity [4]. As stated by Shin *et al.* [5], inter-person variances are used to recognise the identity, while the inter-person variations made by illumination change can be much bigger than the intra-person variations. Many methods have been proposed to handle the illumination problem. However, because of difficulty in controlling the lighting conditions in practical applications, illumination processing is one of the most challenging problems in face recognition.

Over the last decade, many approaches have emerged to tackle the problem of face recognition under varying illumination conditions (Riklin-Raviv [6]; Ramamoorthi [7], 2002; Zhang and Samaras [8]; Wang *et al.* [9]; Zhang and Zhou [10]; Chen *et al.* [11]; Xie and Lam [12]; Phillips *et al.* [13]; Ruiz-del-Solar and Quinteros [3]; Shin *et al.* [5]; Mandal *et al.* [14]; El Aroussi *et al.* [15]; Kao *et al.* [16]; Du and Ward [2]; Fan and Zhang [17]; Hu [18]; just list a few). These approaches can be roughly classified into three main categories: face modelling, normalisation and preprocessing, and invariant feature extraction [3].

Face modelling approaches use low-dimensional linear subspaces to model image variations of human faces under different lighting conditions. They assume that illumination variations are mainly because of the three-dimensional (3D) shape of human faces under lighting in different directions. The linear subspace method considered a human face image as a Lambertian surface [19]. Without ignoring the shadows, the 3D illumination subspace model was extended to a more elaborate model, namely the illumination convex cone [20]. The illumination cone can be approximated in a low-dimensional linear space [21]. Similarly, in the spherical harmonic method, it requires knowledge either about the light source or a large volume of training data [8]. One of the main drawbacks of the face modelling approaches is that for each person, a set of images under different lighting conditions or 3D shape information must be provided to build the linear subspaces. This drawback limits its application in practical face recognition. To deal with the drawback, some related valuable works are proposed. Soyell *et al.* [22] proposed a binary non-subsampled contourlet transform-based illumination robust face representation, where the intrinsic geometrical structures are used for characterising facial texture. Recently, posterior union model (PUM) is used for face recognition with partial occlusion, illumination variation and their combination, assuming no prior information about

the mismatch, and limited training data for each person. PUM is an approach for selecting the optimal local image features for recognition to improve robustness to partial occlusion [23].

At the normalisation and pre-processing stage, image pre-processing algorithms are applied to compensate and normalise illumination. Histogram equalisation is a commonly used method to convert an image to a uniform histogram, which is considered to produce an 'optimal' over contrast in an image. Recently, region-based histogram equalisation and block-based histogram equalisation have been proposed to deal with uneven illumination variations [4, 12]. Most of these algorithms do not require any training or modelling steps, knowledge of 3D face models or reflective surface models. In addition to these algorithms, general-purpose image pre-processing algorithms such as Gamma correction, and logarithmic transforms have also been used for illumination normalisation.

Illumination invariant features are important features in face recognition. In early years, edge maps [24], image intensity derivatives [25] and Gabor-like filters [26] were proposed as illumination invariant features. Unfortunately, these features are not sufficient to overcome image variations because of changes in the direction of lighting [27]. The quotient image was proposed as the illumination invariant signature which can be used for face recognition under varying illumination conditions [28]. The experiment of quotient image showed that the recognition rate of the quotient images outperformed that of the eigenface images. However, this approach usually fails in obtaining the illumination invariant feature when the input image has a shadow. Another efficient tool, the discrete cosine transform (DCT), was used for compensating illumination variations in the logarithmic domain [11].

When we attempt to recognise the identity factor with the new/unkown illumination, we need to translate the new face to the known illumination or translate the known face to the new illumination. This translation procedure requires a repetitive computation of matrix inverse to obtain the identity and illumination factors. This computation may result in a non-convergent case when the observation has noisy information or the model is over fitted. To alleviate this situation, Shin *et al.* [5] proposed a ridge regressive bilinear model which used the ridge regression technique and imposed a penalty to reduce the variance of a certain model. However, which illumination processing methods are good for the advanced feature extraction technique for a given face database remain unknown.

By combining lighting processing with different feature extraction methods, this paper studies how lighting processing affects feature extraction in face recognition. In Section 2, different conventional lighting processing methods are reviewed and compared. In Section 3, two feature extraction methods are proposed. In Section 4, the experimental results are presented and compared with traditional feature extraction methods. Section 5 concludes the paper.

2 Some typical lighting processing methods

In this section, we investigate some typical illumination pre-processing approaches, namely wavelet transformation, self-quotient image, Retinex, smoothing, DCT normalisation in logarithm domain, homomorphic filter and local contrast enhancement.

2.1 Wavelet transform

Wavelet transform is a representation of a signal in terms of a set of basis functions, which is obtained by dilation and translation of a basis wavelet. Wavelet-based image analysis decomposes an image into approximate coefficients and detail coefficients. A normalised image is obtained from the modified coefficients by inverse wavelet transform. The block diagram of the proposed scheme is shown in Fig. 1 [29].

2.2 Self-quotient image

Wang *et al.* [9] present a novel framework, called the self-quotient image, to eliminate lighting effect in the image. This method combines the image processing technique of edge-preserved filtering with the Retinex applications, also see Jobson *et al.* [30] and Gross and Brajovic [31]. The method is shown in Fig. 2. It has two steps: (i) illumination estimation and (ii) the illumination effect subtraction. The self-quotient image Q of image I is defined by

$$Q = \frac{I}{K * I} \tag{1}$$

where K is the smoothing kernel, '*' is the convolution operator and the division is point-wise as in the original quotient image. Q is called the self-quotient image because it is a kind of quotient image derived from the image I itself rather than images of a different person as in QI.

2.3 Multi-scale Retinex

The idea of the Retinex was conceived by Land [32] as a model of the lightness and colour perception of human vision. Its goal is to transform the visual characteristics of the recorded digital image so that the rendition of the transformed image approximates that of the direct observation of scenes. The basic form of the multi-scale

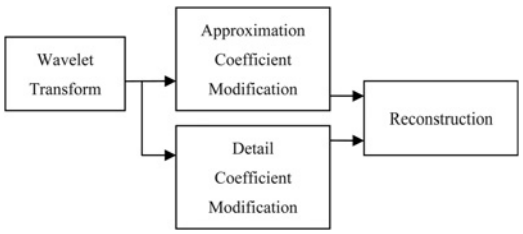

Fig. 1 *Block diagram of the illumination normalisation method*

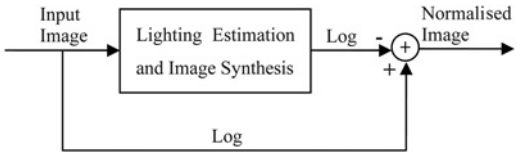

Fig. 2 *Illumination normalisation framework*

Retinex (MSR) is given by

$$R_i(x, y) = \sum_{k=1}^{K} W_k\left(\log I_i(x, y) - \log\left(F_k(x, y) * I_i(x, y)\right)\right)$$
$$i = 1, \ldots, N \tag{2}$$

where the sub-index i represents the ith spectral band, $i \in \{R, G, B\}$ and N is the number of spectral bands. I is the input image, R_i is the output of the MSR process, F_k represents the kth surround function, W_k is the weight associated with F_k and K is the number of surround functions, or scales. The surround function, F_k are given as

$$F_k(x, y) = \kappa \exp\left(-\left(x^2 + y^2\right)/\sigma_k^2\right) \tag{3}$$

where σ_k is the scale that control the extent of the surround and $\kappa = 1/(\Sigma_x \Sigma_y \exp(-(x^2 + y^2)/{\sigma_k}^2))$.

2.4 Anisotropic smoothing

In general, an image $I(x, y)$ acquired by a camera is regarded as the product of two components, reflectance $R(x, y)$ and illumination $L(x, y)$, that is, $I(x, y) = R(x, y)L(x, y)$. Computing the reflectance and the illumination from image, in general, is an ill-posed problem. However, on the assumption that illumination is close to the original image, but contains a smoothing constraint, Gross and Brajovic [31] found an approximate solution of illumination by minimising the following cost function

$$J(L) = \int_{\Omega} \rho(x, y)(L - I)^2 \mathrm{d}x\, \mathrm{d}y + \lambda \int_{\Omega} \left(L_x^2 + L_y^2\right) \mathrm{d}x\, \mathrm{d}y \tag{4}$$

where Ω refers to the image, λ controls the relative importance of the two terms and $\rho(x, y)$ controls the anisotropic properties of smoothing constraint.

2.5 Homomorphic filtering

Illumination-reflectance model (Horn [33]) can be used to develop a frequency-domain approach to improve the appearance of an image by grey-level range compression and contrast enhancement simultaneously. According to this model, each pixel value $I(x, y)$ can be expressed as the product of an illumination component $L(x, y)$ and a reflectance component $R(x, y)$, namely

$$I(x, y) = R(x, y)L(x, y) \tag{5}$$

Let $J(x, y)$ be the desired enhanced image after filtering. The enhancement approach using the homomorphic filtering is shown in Fig. 3.

2.6 Local contrast enhancement

A face relighting algorithm generally suffers from the trouble of higher time complexity, because the problem is usually formulated as an energy minimisation with a few constraints. Two common techniques have been developed to enhance image contrast: global histogram equalisation and local contrast enhancement (LCE). Global histogram equalisation gains the advantage of low complexity and preserves the overall impression of brightness. However, condensing the data range in global view may not effectively enhance fine image textures. LCE efficiently improves visibility of the fine textures. Instead of using the original pixel intensity value, a pixel value is represented by the local contrast, which is the ratio of the intensity of the pixel to the average of its surrounding pixels, in logarithm domain. The dynamic range of the image data has also been compressed. Since the value of local contrast may be positive or negative, data normalisation is necessary.

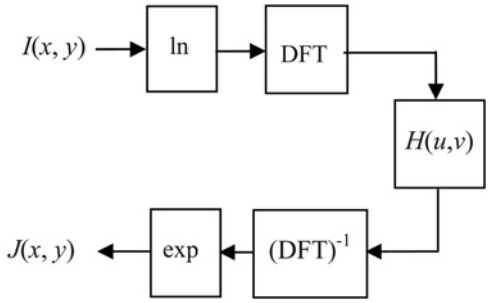

Fig. 3 *Flowchart of homomorphic filtering*

3 Proposed feature extraction methods

In this section, we propose two feature extraction methods, namely adaptive feature extraction (AFE) based on curvelet transform, and the 2D principal component analysis (2DPCA) combined with non-parametric analysis of 2D subspace (2DNSA).

3.1 AFE based on curvelet transform

3.1.1 Curvelet transform: Wavelets and related classical multi-resolution methods use a limited dictionary made up of nearly isotropic elements occurring at all scales and locations. Curvelet is one of such transforms that can efficiently represent edge discontinuities in images. Owing to its anisotropic behaviour, curvelets are elongated needle shaped structures. Owing to this needle shaped structures, curvelets approximate edges by contiguous elongated structures rather than fat dots as wavelets. Consequently, edges can be represented by far less curvelet coefficients compared to wavelets. In other words, curvelets is sparser than wavelets for the same image.

The curvelet transform is a combination of the 2D wavelet transform and the ridgelet transform. The original image is decomposed into a two-dimension wavelet, and each subband is partitioned into $n \times n$ blocks. The ridgelet transform is then applied to each block.

The continuous curvelet transform can be defined by a pair of windows $W(r)$ (a radial window) and $V(t)$ (an angular window), where W is a frequency-domain variable, r and θ are polar coordinates in the frequency domain

$$\sum_{j=-\infty}^{\infty} W^2(2^j r) = 1, \quad r \in \left(\frac{3}{4}, \frac{3}{2}\right) \tag{6}$$

$$\sum_{l=-\infty}^{\infty} V^2(t - l) = 1, \quad t \in \left(-\frac{1}{2}, \frac{1}{2}\right) \tag{7}$$

doi: 10.1049/iet-ipr.2013.0006

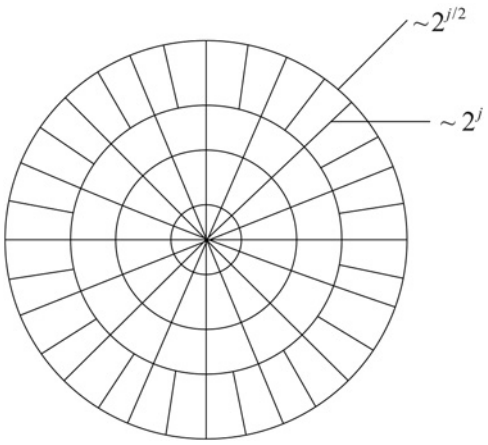

Fig. 4 *Continuous curvelet transform frequency domain*

A polar 'wedge', U_j, as shown in Fig. 4, is defined in the Fourier domain by

$$U_j(r,\theta) = 2^{-3j/4} W(2^{-j}r) V\left(\frac{2^{\lfloor j/2 \rfloor}\theta}{2\pi}\right) \tag{8}$$

Define the waveform $\varphi_j(x)$ by means of its Fourier transform $\varphi_j(\omega) = U_j(\omega)$. The curvelet transform can be defined as a function of $x = (x_1, x_2)$ at scale 2^j, orientation θ_t, and position $x_k^{(j,l)}$ by

$$\varphi_{j,l,k}(x) = \varphi_j\left(R_{\theta_l}\left(x - x_k^{(j,l)}\right)\right) \tag{9}$$

where R_θ is the rotation in radians.

In Fig. 4, the frequency domain is smoothly divided into different angles. This division does not fit the image shape of the 2D Cartesian coordinate. Therefore, it usually uses the same central rectangle area instead of the ring, as shown in Fig. 5.

Define the local window in the Cartesian coordinate by

$$\bar{U}_j(\omega) = \tilde{W}_j(\omega) V_j(\omega) \tag{10}$$

where

$$\tilde{W}_j(\omega) = \sqrt{\Phi_{j+1}^2(\omega) - \Phi_j^2(\omega)} \tag{11}$$

$$V_j(\omega) = V\left(2^{\lfloor j/2 \rfloor}\omega_2/\omega_1\right) \tag{12}$$

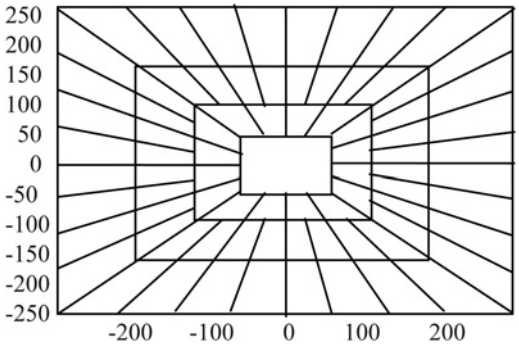

Fig. 5 *Continuous curvelet transform frequency domain*

where Φ is defined as

$$\Phi_j(\omega_1, \omega_2) = \phi\left(2^{-j}\omega_1\right)\phi\left(2^{-j}\omega_2\right) \tag{13}$$

The function ϕ obeys $0 \le \phi \le 1$, might be equal to 1 on $[-1/2, 1/2]$, and vanishes outside of $[-2, 2]$.

By introducing the equal interval slope sequence $\tan\theta_l = l \times 2^{\lfloor -j/2 \rfloor}$, $l = -2^{\lfloor -j/2 \rfloor}, \ldots, 2^{\lfloor -j/2 \rfloor} - 1$, we have

$$\bar{U}_{j,l}(\omega) = \tilde{W}_j(\omega) V_j(S_{\theta_l}\omega) \tag{14}$$

where S_{θ_l} is a cut matrix defined as

$$S_{\theta_l} = \begin{pmatrix} 1 & 0 \\ -\tan\theta & 1 \end{pmatrix} \tag{15}$$

3.1.2 Adaptive feature extraction: Usually, different sets of images have different external environment, such as lighting, background and so on. They also have different internal environment, such as colour, gesture and so on. Therefore, for different databases, different feature selection methods should be used. By training samples according to their adaptive characteristics, the most discriminating features for classification are extracted. For images obtained after the crude curvelet transform, coefficients of scales in different directions are different. To achieve both local and global effects, statistical methods can be used to find the statistical parameters of the region as a feature.

Garcia *et al.* [29] proposed a new method for face recognition based on a wavelet packet decomposition of the face images. Each face image is described by a subset of band filtered images containing wavelet coefficients. The drawback is that the characteristic dimension is too high, which leads to a large computational complexity, and there is too much redundant information. For example, for an image of size 64×64, after curvelet transform by three scales and decomposition of eight directions, we obtain its coefficients with 24 small factors. In accordance to a subblock of size 7×7, there is a total of 537 subblocks. Each subblock is characterised by three statistical parameters. The final feature vector is with 537 dimensions. It is very time consuming. On the other hand, with the mean and variance of light conditions characterised by complex images, redundant information and instability are two problems which are impossible to be neglected.

To overcome the shortcomings of conventional methods and avoid the high dimensionality, we propose to calculate the block entropy of curvelet coefficients. The entropy values are arranged into column vectors which would be used as candidate feature vectors. As the candidate feature vectors may still have redundant information, it is necessary to do feature selection further.

Neither has any candidate eigenvalue the same recognition ability, nor are all candidate features necessary for recognition. To improve the recognition accuracy, it is necessary to analysis the recognition abilities of different features and build up the feature vector based on those features with high recognition abilities. Similar to the LDA method, this paper select features which make within-class distance small and between-class distance large. Variance is used to measure the dispersion of the data set. The ratio of within-class variance to between-class variance is used to measure the recognition ability of the candidate feature.

For a given training set, suppose it has C classes, each class has S samples and k features are selected for face recognition.

Let $\boldsymbol{A} = [\boldsymbol{A}_1, \ldots, \boldsymbol{A}_k]$ denote the training set of candidate feature matrix for all samples, where

$$\boldsymbol{A}_i = \begin{pmatrix} x_i(1, 1) & \cdots & x_i(1, C) \\ \cdots & \cdots & \cdots \\ x_i(S, 1) & \cdots & x_i(S, C) \end{pmatrix} \tag{16}$$

i indicates the ith candidate characteristic matrix of all training samples, $i = 1, \ldots, k$. $x_i(p, q)$ represents the ith candidate eigenvalue of the qth sample in the pth class. The steps to obtain the estimation value of identifying factors for any candidate eigenvalue are described as follows:

Step 1: Compute the within-class mean value for each feature in every class

$$M_i^l = \frac{1}{S}\sum_{j=1}^{S} A_i(j, l), \quad l = 1, \ldots, C; \quad i = 1, \ldots, k \tag{17}$$

Step 2: Compute the within-class variance

$$V_i^l = \sum_{j=1}^{S}\left(A_i(j, l) - M_i^l\right)^2, \quad l = 1, \ldots, C; \quad i = 1, \ldots, k \tag{18}$$

$$V_i^{\mathrm{W}} = \frac{1}{C}\sum_{l=1}^{C} V_i^l; \quad i = 1, \ldots, k \tag{19}$$

Step 3: Compute the between-class mean value

$$M_i = \frac{1}{S \times C}\sum_{l=1}^{C}\sum_{j=1}^{S} A_i(j, l); \quad i = 1, \ldots, k \tag{20}$$

Step 4: Compute the between-class variance

$$V_i^{\mathrm{B}} = \sum_{l=1}^{C}\sum_{j=1}^{S}\left(A_i(j, l) - M_i^l\right)^2; \quad i = 1, \ldots, k \tag{21}$$

Step 5: Compute the estimation of identification ability

$$D_i = \frac{V_i^{\mathrm{B}}}{V_i^{\mathrm{W}}}, \quad i = 1, \ldots, k \tag{22}$$

Finally, by sorting estimation in descent order, we obtain the candidates from strong to weak characteristics of the index value, which finish the feature selection.

3.2 2DPCA and 2DNSA

To overcome the 'small sample size' problem, a projection technique is performed through two-directional and 2D approach which simultaneously work in row and column directions. In this section, we investigate two such techniques, namely the 2DPCA [34], and the 2DNSA. Other popular 2D feature extraction methods can be found in literatures, such as the 2D linear discriminant analysis (2DLDA) [35], the two-directional and 2DPCA ((2D)^{2}PCA) [10], the two-directional and 2DLDA ((2D)^{2}LDA) [36].

3.2.1 2D principal component analysis: Suppose there are $\boldsymbol{N}$ training samples $A_i (i = 1, \ldots, N) \in R^{m \times n}$, which belongs to K classes, N_i denotes the number of samples in the ith class. The total number of samples is $N = \sum_{i=1}^{C} N_i$. Let $\boldsymbol{X} \in R^{n \times d}$ be the orthonormal column matrix, and $n \geq d$. Projecting $\boldsymbol{A}_i$ by $\boldsymbol{X}$, we have $\boldsymbol{Y}_i = \boldsymbol{A}_i\boldsymbol{X} \in R^{m \times d}$. Like in PCA, denote ε as the mathematical expectation, and

$$\begin{aligned} \boldsymbol{J}(\boldsymbol{X}) &= \mathrm{trace}\left\{\mathcal{E}\left[(\boldsymbol{Y} - \mathcal{E}\boldsymbol{Y})(\boldsymbol{Y} - \mathcal{E}\boldsymbol{Y})^{\mathrm{T}}\right]\right\} \\ &= \mathrm{trace}\left\{\boldsymbol{X}^{\boldsymbol{T}}\mathcal{E}\left[(\boldsymbol{A} - \mathcal{E}\boldsymbol{A})(\boldsymbol{A} - \mathcal{E}\boldsymbol{A})^{\mathrm{T}}\right]\boldsymbol{X}\right\} \end{aligned} \tag{23}$$

Denote

$$\boldsymbol{G} = \left\{\mathcal{E}\left[(\boldsymbol{A} - \mathcal{E}\boldsymbol{A})(\boldsymbol{A} - \mathcal{E}\boldsymbol{A})^{\mathrm{T}}\right]\right\} \tag{24}$$

then $\boldsymbol{G}$ is a non-negative definite matrix and $\boldsymbol{G} \in R^{n \times n}$. Generally, we use the average images to obtain $\boldsymbol{G}$

$$\boldsymbol{G} = \frac{1}{N}\sum_{k=1}^{N}\left(\boldsymbol{A}_k - \bar{\boldsymbol{A}}\right)\left(\boldsymbol{A}_k - \bar{\boldsymbol{A}}\right)^{\mathrm{T}} \tag{25}$$

where

$$\bar{\boldsymbol{A}} = \frac{1}{N}\sum_{k=1}^{N}\boldsymbol{A}_k \tag{26}$$

Extracting features by decomposition of $\boldsymbol{G}$, eigenvectors corresponding to the first d largest eigenvalues constitute the optimal projection matrix $\boldsymbol{X}_{\mathrm{opt}} = [\boldsymbol{X}_1, \ldots, \boldsymbol{X}_d]$. d is determined by

$$\frac{\sum_{i=1}^{d}\lambda_i}{\sum_{i=1}^{n}\lambda_i} \geq \theta \tag{27}$$

where $\lambda_1, \ldots, \lambda_d$ are the first d largest eigenvalues of $\boldsymbol{G}$ and θ is a given threshold.

3.2.2 2D non-parametric space analysis: After 2DPCA processing, the original high-dimensional image matrix becomes a low-dimensional matrix, then the training sample set of images is mapped into $\boldsymbol{Y}_i (i = 1, \ldots, N) \in R^{m \times d}$, with C classes. Similar to the change from PCA to 2DPCA, this paper changes the NSA to 2DNSA. Within-class scatter matrix and between-class scatter matrix are defined as follows

$$S_{\mathrm{w}}^{\mathrm{2DNSA}} = \sum_{i=1}^{C}\sum_{l=1}^{N_i}\left(\boldsymbol{Y}_1^{\mathrm{i}} - \bar{\boldsymbol{Y}}_i\right)\left(\boldsymbol{Y}_1^{\mathrm{i}} - \bar{\boldsymbol{Y}}_i\right)^{\mathrm{T}} \tag{28}$$

$$\begin{aligned} S_{\mathrm{b}}^{\mathrm{2DNSA}} = &\sum_{i=1}^{C}\sum_{j=1, j\neq i}^{C}\sum_{l=1}^{N_i} w(i, j, l)\left(\boldsymbol{Y}_1^{\mathrm{i}} - \mathrm{m}_j\left(\boldsymbol{Y}_1^{\mathrm{i}}\right)\right) \\ &\times \left(\boldsymbol{Y}_1^{\mathrm{i}} - \mathrm{m}_j\left(\boldsymbol{Y}_1^{\mathrm{i}}\right)\right)^{\mathrm{T}} \end{aligned} \tag{29}$$

where C is the number of classes, N_i is the total number of samples in the ith class, $\boldsymbol{Y}_1^{\mathrm{i}}$ is the lth vector in the ith class, $m_j(\boldsymbol{Y}_l^i)$ is k-mean vector in the local neighbours of the samples in the jth class, and $w(i, j, l)$ is the weight

doi: 10.1049/iet-ipr.2013.0006

function, which is defined as

$$w(i, j, l) = \frac{\min\left(d^{\alpha}\left(\boldsymbol{Y}_l^i, \boldsymbol{NN}_k\left(\boldsymbol{Y}_l^i, i\right)\right), d^{\alpha}\left(\boldsymbol{Y}_l^i, \boldsymbol{NN}_k\left(\boldsymbol{Y}_l^i, j\right)\right)\right)}{d^{\alpha}\left(\boldsymbol{Y}_l^i, \boldsymbol{NN}_k\left(\boldsymbol{Y}_l^i, i\right)\right) + d^{\alpha}\left(\boldsymbol{Y}_l^i, \boldsymbol{NN}_k\left(\boldsymbol{Y}_l^i, j\right)\right)} \tag{30}$$

where

$$m_j\left(\boldsymbol{Y}_l^i\right) = \frac{1}{k}\sum_{p=1}^{k} \boldsymbol{NN}_p\left(\boldsymbol{Y}_l^i, j\right) \tag{31}$$

$$Y^i = \frac{1}{N_i}\sum_{l=1}^{N_i} \boldsymbol{Y}_l^i \tag{32}$$

where α is a parameter with non-negative value to control the distance ratio of the change. $d(V_1, V_2)$ is the image Euclidean distance between matrix $\boldsymbol{V}_1$ and $\boldsymbol{V}_2$. $\boldsymbol{NN}_p\left(\boldsymbol{Y}_l^i, j\right)$ is the sample matrix in the jth class neighbour sample matrix $\boldsymbol{Y}_l^i$. Finally, by matrix decomposition on $\left(\boldsymbol{S}_{\mathrm{w}}^{\mathrm{2DNSA}}\right)^{-1}\boldsymbol{S}_{\mathrm{b}}^{\mathrm{2DNSA}}$, we obtain the best projection matrix $\boldsymbol{Z}_{\mathrm{opt}} = [\boldsymbol{Z}_1, \ldots, \boldsymbol{Z}_q]$, which is corresponding to the top q largest eigenvalues.

3.2.3 Feature extraction and classification: After dimension reduction, pre-2DPCA and 2DNSA feature extraction, the final feature matrix is given as follows

$$T = \boldsymbol{Z}_{\mathrm{opt}}^{\mathrm{T}}\boldsymbol{A}\boldsymbol{X}_{\mathrm{opt}} \tag{33}$$

For a given test image matrix $\boldsymbol{A}'$, suppose its feature matrix is $\boldsymbol{T}'$ by (33). By using the cosine distance classifier, the corresponding class can be found

$$d_{\cos}(\boldsymbol{T}', \boldsymbol{T}) = \frac{\boldsymbol{T}'\boldsymbol{T}}{\|\boldsymbol{T}'\|\|\boldsymbol{T}\|} \tag{34}$$

4 Experimental results

In order to study how lighting processing effects on feature extraction and face recognition rate, we use seven public face databases for the purpose of experimental verification and analysis. We present experiments to compare different lighting processing methods, including non-processing (NP), wavelet normalisation (WN), single scale self-quotient image (SSQI), multi-scale self-quotient image (MSQI), single scale Retinex (SSR), multi-scale Retinex (MSR), adaptive single scale Retinex (ASSR), anisotropic smoothing (AS), homomorphic filtering (HF), LCE and the proposed curvelet transform (CT). Also we present experimental comparison of 2D matrix-based feature extraction methods, including 2DPCA, 2DLDA, $(2D)^2$PCA, $(2D)^2$LDA and non-parametric 2DPCA subspace analysis (2DPCA + 2DNSA).

4.1 Face databases and samples

The Yale face database was collected by the Yale Center for Computation Vision and Control [37]. There are 165 images of 15 individuals in Yale face data sets. Each person has 11 different images. The images demonstrate variations in lighting condition (left-light, centrE-light and right-light), facial expression (normal, happy, sad, sleepy, surprised and wink) and with or without glasses. All samples were normalised to the image resolution of 80×80. In this experiment, 3 images per person are randomly selected as training samples, and the remaining eight as testing samples. That is, 45 training samples, 120 test samples.

The ORL face database contains a set of face images taken between April 1992 and April 1994 in the lab [38]. There are 40 distinct faces and each of them has 10 different images. The size of each image is 92×112 pixels, with 256 grey levels per pixel. In the experiment, all samples were normalised to the image resolution of 80×80. For each person, three images are randomly selected as training samples, and the remaining seven are used as the test samples. That is, 120 training samples and 280 test samples.

The CAS-PEAL face database is constructed under the sponsors of National Hi-Tech Program and ISVISION by the Face Recognition Group of JDL, ICT, CAS [39]. Currently, the CAS-PEAL face database contains 99 594 images of 1040 individuals (595 males and 445 females) with varying Pose, Expression, Accessory, and Lighting (PEAL). This face database is now partly available (a subset named by CAS-PEAL-R1, contain 30 900 images of 1040 subjects) for research purpose on a case-by-case basis only.

The CMU PIE face database includes 68 subjects with 41 368 face images as a whole. For each background illumination and pose, each person was taken of 21 images, including 8 images with flash and face centre in the same plane and a negative face placed from $-90°$ to $+90°$, and 13 images with flash in the face side (or top of the ramp) and the human face into poses between about $-67.5°$ to $+67.5°$. Each image implies changes in the expression for the normal expression, smile and blink. This database can be found in [40].

4.2 Experiments on AFE-based curvelet transform

In order to verify that the proposed method is reliable and easy to implement, we use the following four individuals face databases for experimental verification, namely, Yale, ORL, CAS-PEAL and CMU PIE face database. Before proceeding the experiment, all images are normalised to the same size. In order to verify block entropy BE (Block Entropy), we constitute the candidate eigenvectors based on curvelet transform domain coefficients. The specific experimental procedure is as follows:

1. Randomly select several images as training from image database, the remaining for testing. In this experiment, we randomly select 3 images per person from Yale database as training, and 8 images as test samples; 3 images per person from ORL database as training, and 7 images as test samples; 3 images per person from CAS-PEAL database as training, and 7 images as test samples; 80 images per person from CMU PIE database as training, and 90 images as test samples.
2. For all images, we use the local contrast enhancement processing. Local area is of size 5×5.
3. Run curvelet transform on images, obtain the transform coefficients.
4. Compute the block entropy corresponding to their transform coefficients, and arrange all the entropy values in a vector which constitutes the candidate feature.
5. Classify, test and verify based on the minimum distance.

The experimental results are listed in Table 1. For each data item, there is a lighting processing method on top of it, which

Table 1 Face recognition rate with AFE based on curvelet transform

		2DPCA	$(2D)^2$PCA	2DLDA	$(2D)^2$ LDA	AFE
Yale	best LP	SSR	MSR	MSQI	MSQI	LCE
	accuracy	0.9550	0.9725	0.9750	0.9804	0.9753
ORL	best LP	NP	NP	WN	NP	LCE
	accuracy	0.8811	0.8793	0.9175	0.9196	0.9338
CAS-PEAL	best LP	NP	NP	NP	NP	LCE
	accuracy	0.7964	0.7843	0.8814	0.9221	0.9300
CMU PIE	best LP	ASSR	MSQI	WN	MSQI	LCE
	accuracy	0.9676	0.9816	0.9781	0.9899	0.9875

represents the best lighting processing method based on the given feature extraction method.

Table 1 shows that the proposed method, AFE based on curvelet transform, has good performance in face recognition for the given four databases, comparing with the other feature extraction techniques. Especially, for ORL and CAS-PEAL face databases, the proposed method performs better than the other two traditional feature extraction methods. There is little space to improve the recognition rate.

4.3 Experiments on 2DPCA non-parameter subspace analysis

In order to study 'how illumination pretreatment methods affect feature extraction for different face databases', we set up the experiments for five different feature extraction methods, respectively. For each feature extraction method, experimental results of face recognition accuracy are listed in Tables 2–6, including nine illumination pretreatment methods and the non-pretreatment on four face databases. For each feature extraction method, there are two corresponding columns in the table. One column shows the face recognition accuracy. We use '(0)' to denote that there is no illumination pretreatment, '(+)' to denote that the illumination pretreatment improves the recognition accuracy, and '(−)' to denote the decrease of the accuracy. In this way, the table shows which illumination pretreatment method is efficient while combining with the feature extraction method for the given face database.z

Meanwhile, in order to eliminate the interference involved by random choice of samples, each item as the recognition accuracy is an average value which is computed by ten random times of tests. To illustrate it, we give an example to show how we compute the accuracy for a feature extraction method combined with different lighting processing, as shown in Fig. 6. For each combination of feature extraction and lighting processing, there are ten random face recognition data which constructs one type of line as denoted in the legend.

Table 2 shows the experimental results of face recognition accuracy corresponding to the 2DPCA feature extraction, combined with nine illumination pretreatment methods on the given face databases. The first row corresponding to the non-pretreatment gives the face recognition accuracy without lighting processing.

Table 2 shows that 2DPCA is effective in face recognition for the Yale and CMU PIE databases by arranging lighting processing for most cases. In detail, for Yale database, five out of nine lighting processing methods are good in increasing face recognition accuracy, and the SSR lighting processing method has the best performance. Although for CMU PIE database, seven out of nine lighting processing methods are efficient in helping 2DPCA to improve the recognition accuracy, and the ASSR method performs the best.

Table 2 Face recognition rate comparison for 2DPCA feature extraction

Lighting processing	Yale	ORL	CAS-PEAL	CMU PIE
NP	0.9433(0)	0.8811(0)	0.7964(0)	0.9350(0)
WN	0.9483(+)	0.8682(−)	0.7921(−)	0.9637(+)
SSQI	0.9450(+)	0.7786(−)	0.7200(−)	0.9617(+)
MSQI	0.9450(+)	0.8211(−)	0.7514(−)	0.9581(+)
SSR	**0.9550**(+)	0.8550(−)	0.5921(−)	0.8891(−)
MSR	0.9492(+)	0.8425(−)	0.5821(−)	0.8937(−)
ASSR	0.8083(−)	0.7571(−)	0.7186(−)	**0.9676** (+)
AS	0.9000(−)	0.4607(−)	0.6164(−)	0.9429(+)
HF	0.8600(−)	0.6200(−)	0.6493(−)	0.9553(+)
LCE	0.7317(−)	**0.2814**(−)	**0.5264**(−)	0.9485(+)

'(0)' to denote that there is no illumination pretreatment, '(+)' to denote that the illumination pretreatment improves the recognition accuracy and '(−)' to denote the decrease of the accuracy.

Table 3 Face recognition rate comparison for $(2D)^2$PCA feature extraction

Lighting processing	Yale	ORL	CAS-PEAL	CMU PIE
NP	0.9175(0)	0.8793(0)	0.7843(0)	0.9637(0)
WN	0.9437(+)	0.8586(−)	0.7464(−)	0.9767(+)
SSQI	0.9717(+)	0.8018(−)	0.6839(−)	0.9790(+)
MSQI	0.9687(+)	0.8218(−)	0.6954(−)	**0.9816**(+)
SSR	0.9692(+)	0.8641(−)	0.5961(−)	0.9352(+)
MSR	**0.9725**(+)	0.8575(−)	0.5964(−)	0.9427(+)
ASSR	0.7875(−)	0.7702(−)	0.6800(−)	0.9807(+)
AS	0.8792(−)	0.4470(−)	0.5929(−)	0.9530(+)
HF	0.8637(−)	0.6912(−)	0.6271(−)	0.9689(+)
LCE	0.8300(−)	**0.3257**(−)	**0.5132**(−)	0.9746(+)

'(0)' to denote that there is no illumination pretreatment, '(+)' to denote that the illumination pretreatment improves the recognition accuracy and '(−)' to denote the decrease of the accuracy.

For ORL and CAS-PEAL face databases, their performances are worse than the case without lighting processing. Some lighting processing techniques, such as LCE, ansitropic smoothing, even decrease the face recognition accuracy deeply for ORL database. So is the LCE, which has bad performance for 2DPCA on the CAS-PEAL database.

Similarly, from Tables 3–6, we present the experimental results of face recognition for the other four feature

doi: 10.1049/iet-ipr.2013.0006

Table 4 Face recognition rate comparison for 2DLDA feature extraction

Lighting processing	Yale	ORL	CAS-PEAL	CMU PIE
NP	0.9358(0)	0.9136(0)	0.8814(0)	0.9611(0)
WN	0.9658(+)	0.9175(+)	0.8300(–)	**0.9781**(+)
SSQI	0.9650(+)	0.8479(–)	0.7779(–)	0.9636(+)
MSQI	**0.9750**(+)	0.8725(–)	0.7793(–)	0.9653(+)
SSR	0.9733(+)	0.8736(–)	0.6171(–)	0.9229(–)
MSR	0.9683(+)	0.8711(–)	0.5914(–)	0.9215(–)
ASSR	0.8992(–)	0.8589(–)	0.7600(–)	0.9680(+)
AS	0.9533(+)	0.6239(–)	0.7314(–)	0.9445(–)
HF	0.9192(–)	0.6779(–)	0.7321(–)	0.9541(–)
LCE	0.8308(–)	**0.4150**(–)	0.6143(–)	0.9544(–)

'(0)' to denote that there is no illumination pretreatment, '(+)' to denote that the illumination pretreatment improves the recognition accuracy and '(–)' to denote the decrease of the accuracy.

Table 5 Face recognition rate comparison for $(2D)^2$LDA feature extraction

Lighting processing	Yale	ORL	CAS-PEAL	CMU PIE
NP	0.9192(0)	0.9196(0)	0.9221(0)	0.9827(0)
WN	0.9300(+)	0.9057(–)	0.8957(–)	**0.9897**(+)
SSQI	0.9654(+)	0.8496(–)	0.8221(–)	0.9871(+)
MSQI	**0.9804**(+)	0.8698(–)	0.8311(–)	0.9899(+)
SSR	0.9742(+)	0.8788(–)	0.6839(–)	0.9806(–)
MSR	0.9671(+)	0.8689(–)	0.7114(–)	0.9798(–)
ASSR	0.8904(–)	0.8498(–)	0.7482(–)	0.9873(+)
AS	0.9408(+)	0.5959(–)	0.7204(–)	0.9813(–)
HF	0.9254(+)	0.7795(–)	0.7493(–)	0.9800(–)
LCE	0.8829(–)	**0.5045(–)**	**0.6957(–)**	0.9760(–)

'(0)' to denote that there is no illumination pretreatment, '(+)' to denote that the illumination pretreatment improves the recognition accuracy and '(–)' to denote the decrease of the accuracy.

Table 6 Face recognition rate comparison for 2DPCA + 2DNSA feature extraction

Lighting processing	Yale	ORL	CAS-PEAL	CMU PIE
NP	0.9750(0)	0.8518(0)	0.9393(0)	0.9380(0)
WN	0.9375(–)	0.8389(–)	0.8779(–)	0.9451(+)
SSQI	0.9825(+)	0.7668(–)	0.8043(–)	0.9233(–)
MSQI	0.9725(–)	0.8014(–)	0.8129(–)	0.9313(–)
SSR	0.9425(–)	0.8146(–)	0.6821(–)	0.8710(–)
MSR	0.9417(–)	0.8014(–)	0.7407(–)	0.9414(+)
ASSR	0.9483(–)	0.7986(–)	0.6607(–)	0.8783(–)
AS	0.9242(–)	0.4111(–)	0.6879(–)	0.9284(–)
HF	0.9417(–)	0.7414(–)	0.7243(–)	0.8657(–)
LCE	0.8650(–)	0.3796(–)	0.5807(–)	0.9473(+)

'(0)' to denote that there is no illumination pretreatment, '(+)' to denote that the illumination pretreatment improves the recognition accuracy and '(–)' to denote the decrease of the accuracy.

extraction methods, combined with nine illumination pretreatment methods on four different face databases.

Very similar to Tables 2 and 3 tell us $(2D)^2$PCA is effective in face recognition for the Yale and CMU PIE databases by introducing lighting processing in most cases. In detail, for Yale database, five out of nine lighting processing methods are good in increasing face recognition accuracy, and the MSR lighting processing method combined with $(2D)^2$PCA has the best performance. Although for CMU PIE database, all lighting processing methods are efficient in helping $(2D)^2$PCA to improve the recognition accuracy. The MSQI method is the best.

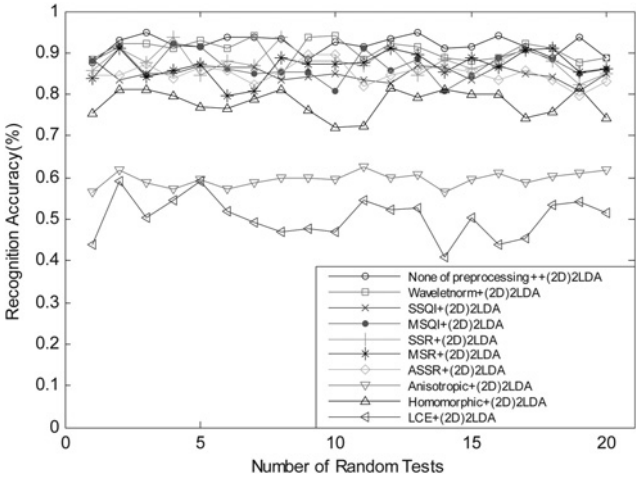

Fig. 6 *Face recognition accuracy for $(2D)^2$LDA on ORL database*

In Tables 2 and 3, all the performances are worse than the case without using lighting processing for ORL and CAS-PEAL face databases. Some lighting processing techniques, such as LCE, even decrease the face recognition accuracy deeply for ORL and CAS-PEAL database.

Table 4 shows that 2DLDA is effective in face recognition for Yale database when combined with most lighting processing methods, except ASSR, HF and LCE. In detail, for Yale database, six out of nine lighting processing methods are good in increasing face recognition accuracy, and the MSQI lighting processing method has the best performance combined with 2DLDA. Although for CMU PIE database, four out of nine lighting processing methods are efficient in helping 2DLDA to improve the recognition accuracy, and the WN method obtains the best results.

However, most of all the lighting processing methods have bad performance with 2DLDA in face recognition accuracy for ORL and CAS-PEAL face databases. This is very similar to the case in Table 2. LCE is the worst in decreasing the face recognition accuracy for ORL database.

Table 5 shows that $(2D)^2$LDA is effective in face recognition for the Yale database when combined with most lighting processing methods, except ASSR, HF and LCE. In detail, for Yale database, seven out of nine lighting processing methods are good in increasing face recognition accuracy, and the MSQI lighting processing method has the best performance combined with 2DLDA. Although for CMU PIE database, four out of nine lighting processing methods are efficient in helping 2DLDA to improve the recognition accuracy, and the WN method reaches the peak.

However, most of all the lighting processing methods have bad performance with 2DLDA in face recognition accuracy for ORL and CAS-PEAL face databases. This is very similar to the case in Table 2. Again, LCE is the worst in decreasing the face recognition accuracy for ORL and CAS-PEAL databases.

Table 6 shows that 2DPCA + DNSA is almost useless when combined with the proposed nine lighting processing methods in face recognition. In detail, only SSOI is effective for 2DPCA + DNSA on the Yale database. Although for the CMU PIE database, three out of nine lighting processing methods can be used for 2DPCA + DNSA in increasing face recognition accuracy, namely, WN, MSR and LCE.

Unexpectedly, 90% of the lighting processing methods have bad performance with 2DPCA + DNSA in face recognition for the four face databases. Hence, we do not suggest using lighting processing methods as a combiner for the feature extraction 2DPCA + DNSA.

If one pays more attention to Table 6, one would find that even without light preprocessing, the results by the 2DPCA + 2DNSA feature extraction method are pretty good. From Table 6, only 10% of cases with lighting preprocessing have positive influence on improving the face recognition rate. It means that the proposed 2DPCA + 2DNSA feature extraction method is stable and robust to different lighting conditions. In fact, lighting preprocessing is not always good. Most light processing methods for face recognition will lose high frequent part of the image signals.

The last five tables show that lighting processing for a comprehensive analysis and feature extraction is necessary on the Yale and CMU PIE face databases, but useless on the ORL and CAS-PEAL face databases. The lighting processing method proposed is neither good nor bad if there is no uniform evaluation criteria. The human visual sensation will be the dominant evaluation factors, and the preprocessed image with better visual experience may not be better face feature. By using image similarity, the pretreatment evaluation would be a preferred method, but simply relying on the similarity of the preprocessed image recognition is not reliable. So the face recognition pretreatment is not only a pre-treatment process, but also a need for further feature extraction.

4.4 Discussions

To show more details of the face recognition results, some image examples of the correctly and incorrectly recognised faces are shown in Figs. 7 and 8. Fig. 7 shows some typical classification results by the proposed method on the Yale database. The first row is the results based on the SSQI lighting processing method and the second row is the results based on the MSR lighting processing method. The left three columns in the green rectangular box are the correctly classified faces and the last column in the red rectangular box are the incorrectly classified faces. The results show that the proposed methods are robust to different illumination conditions. The failure examples are mainly because of occlusions. For example, the face images for the person in the first row are mainly without glasses, so the face image with glasses may be misclassified. On the contrary, if most of the images of a person are with glasses, the same face image without glasses has a relative large possibility to be misclassified.

Some typical classification results by the proposed method on the ORL database are shown in Fig. 3. The first row is the results based on the SSQI lighting processing method and the second row is the results based on the MSR lighting processing method. The left three columns in the green rectangular box are the correctly classified faces and the last column in the red rectangular box are the incorrectly classified faces. The failure examples in the first row are with closed eyes. The misclassified face in the second row is mainly due to the fact that the person slightly lowered his head and turned his head to left.

Table 7 lists the computation times and accuracies by different face recognition methods, on the CAS-PEAL dataset. The MATLAB codes were run on one core of a Core Duo 2.5 GHz desktop with 2GB of memory running Windows XP professional. From this table, one may find that the proposed 2DPCA + 2DNSA method takes less time than other methods, and the accuracy is higher than other methods.

Fig. 7 *Some image examples of the correctly recognised faces (left three columns) and incorrectly identified faces (the last column) by the proposed method on the Yale database*

The first row is the results based on the SSQI lighting processing method and the second row is the results based on the MSR lighting processing method

doi: 10.1049/iet-ipr.2013.0006

Fig. 8 *Some image examples of the correctly classified faces (left three columns) and incorrectly classified faces (the last column) by the proposed method on the ORL database*

The first row is the results based on the SSQI lighting processing method and the second row is the results based on the MSR lighting processing method

Table 7 Face recognition accuracy (%) and execution time (second) by different methods, on the CAS-PEAL dataset

Dimension of feature vectors	4		6		8		10	
Time and accuracy	Time	Accuracy	Time	Accuracy	Time	Accuracy	Time	Accuracy
$(2D)^2PCA$	0.1775	69.71	0.1844	75.89	0.1868	79.96	0.1979	79.96
2DPCA	0.1907	81.14	0.2000	80.57	0.2064	82.82	0.2281	81.54
$(2D)^2LDA$	0.1850	87.46	0.1883	91.86	0.1944	92.36	0.2023	92.96
2DLDA	0.1931	88.71	0.2048	89.68	0.2140	88.64	0.2242	88.89
2DPCA + 2DNSA	0.1436	89.07	0.1453	93.00	0.1482	93.36	0.1524	92.94

5 Conclusion

This paper investigates some lighting processing methods for face recognition. The studies also show how different lighting conditions affect face recognition based on different feature extraction methods. Based on curvelet transform, an adaptive robust face recognition feature extraction method is proposed. By combining the curvelet transform with the AFE, face recognition rate can be improved efficiently.

The main contribution of this paper is that a non-parametric 2D PCA sub-space analysis method, called 2DPCA + 2DNSA method, is proposed for feature extraction for face recognition. Experiments on different benchmark datasets are presented and compared in this paper. The experiment results show that the AFE method based on curvelet transform outperforms conventional methods. The experiment results also show that the 2DPCA + 2DNSA feature extraction method is stable and robust to different lighting conditions.

6 Acknowledgment

This work is supported by the Blue Project of Universities in Jiangsu Province Training Young Academic Leaders Object, and National Natural Science Foundation of China (no. 61170121). The authors would like to thank the online face database providers including Yale, Yale B, ORL, AR, CAS-PEAL and CMU PIE.

7 References

1 Zhang, X., Gao, Y.: 'Face recognition across pose: a review', *Pattern Recognit.*, 2009, **42**, (11), pp. 2876–2896
2 Du, S., Ward, R.K.: 'Adaptive region-based image enhancement method for robust face recognition under variable illumination conditions', *IEEE Trans. Circuits Syst. Video Technol.*, 2010, **20**, pp. 1165–1175
3 Ruiz-del-Solar, J., Quinteros, J.: 'Illumination compensation and normalization in eigenspace-based face recognition: a comparative study of different pre-processing approaches', *Pattern Recognit. Lett.*, 2008, **29**, pp. 1966–1979
4 Xie, X., Lam, K.M.: 'Face recognition under varying illumination based on a 2D face shape model', *Pattern Recognit.*, 2005, **38**, pp. 221–230
5 Shin, D., Lee, H.-S., Kim, D.: 'Illumination-robust face recognition using ridge regressive bilinear modes', *Pattern Recognit. Lett.*, 2008, **29**, pp. 49–58
6 Riklin-Raviv, T.: 'The quotient image: class-based re-rendering and recognition with varying illuminations', *IEEE Trans. Pattern Anal. Mach. Intell.*, 2001, **23**, pp. 129–139
7 Ramamoorthi, R.: 'Analytic PCA construction for theoretical analysis of lighting variability in images of a Lambertian object', *IEEE Trans. Pattern Anal. Mach. Intell.*, 2002, **24**, pp. 1322–1333
8 Zhang, L., Samaras, D.: 'Face recognition under variable lighting using harmonic image exemplars'. Proc. of IEEE Conf. on Computer Vision and Pattern Recognition, 2003, vol. 1, pp. 19–25
9 Wang, H., Li, S., Wang, Y.: 'Face recognition under varying lighting conditions using self-quotient image'. Proc. Sixth Int. Conf. on Face and Gesture Recognition, Pattern Recognition Letters, 2004, vol. 27, pp. 609–617
10 Zhang, D., Zhou, Z.-H.: '$(2D)^2PCA$: two-directional two-dimensional PCA for efficient face representation and recognition', *Neurocomputing*, 2005, **69**, pp. 224–231
11 Chen, T., Zhou, X.S., Comaniciu, D., Huang, T.S.: 'Total variation models for variable lighting face recognition', *IEEE Trans. Pattern Anal. Mach. Intell.*, 2006, **28**, pp. 1519–1524
12 Xie, X., Lam, K.M.: 'An efficient illumination normalization method for face recognition', *Pattern Recognit. Lett.*, 2006, **27**, pp. 609–617

13 Phillips, J., Scruggs, T., O'Toole, A., *et al*..: '2007, FRVT 2006 and ICE 2006 large-scale results'. NISTIR 7408 Report, March 2007
14 Mandal, T., Wu, Q.M., Yuan, Y.: 'Curvelet based face recognition via dimension reduction', *Signal Process.*, 2009, **89**, pp. 2345–2353
15 El Aroussi, M., Ghouzali, S., El Hassouni, M., Rziza, M., Aboutajdine, D.: 'Block based curvelet feature extraction for face recognition'. Int. Conf. on Multimedia Computing and Systems, ICMCS, 2009, pp. 299–303
16 Kao, W.-C., Hsu, M.-C., Yang, Y.-Y.: 'Local contrast enhancement and adaptive feature extraction for illumination invariant face recognition', *Pattern Recognit.*, 2010, **43**, pp. 1736–1747
17 Fan, C.-N., Zhang, F.-Y.: 'Homomorphic filtering based illumination normalization method for face recognition', *Pattern Recognit. Lett.*, 2011, **32**, pp. 1468–1479
18 Hu, H.: 'Variable lighting face recognition using discrete wavelet transform', *Pattern Recognit. Lett.*, 2011, **32**, pp. 1526–1534
19 Hallinan, P.W.: 'A low-dimensional representation of human faces for arbitrary lighting conditions'. Proc. IEEE Conf. CVPR, Seattle, 1994
20 Belhumeur, P.N., Kriegman, D.J.: 'What is the set of images of an object under all possible lighting conditions?'. Proc. of IEEE Conf. on Computer Vision and Pattern Recognition, 1996, pp. 270–277
21 Basri, R., Jacobs, D.W.: 'Lambertian reflectance and linear subspaces', *IEEE Trans. Pattern Anal. Mach. Intell.*, 2003, **25**, pp. 218–233
22 Soyell, H., Ozment, B., McOwant, P.W.: 'Illumination robust face representation based on intrinsic geometrical information'. IET Image Processing Conf. 2012, University of Westminster, London, UK, 3–4 July 2012
23 Lin, J., Ji, M., Crookes, D.: 'Robust face recognition with partial occlusion, illumination variation and limited training data by optimal feature selection', *IET Comput. Vis.*, 2011, **5**, pp. 23–32
24 Govindaraju, V., Sher, D.B., Srihari, R., Srihari, S.N.: 'Locating human faces in newspaper photographs'. Proc. IEEE Conf. on Computer Vision Pattern Recognition, 1989, pp. 549–554
25 Edelman, S., Reisfeld, D., Yeshurun, Y.: 'A system for face recognition that learns from examples'. Proc. Eur. Conf. on Computer Vision, 1992, pp. 787–791
26 Daugman, J.G.: 'Uncertainty relation for resolution in space, spatial frequency and orientation optimized by 2-D cortical filters', *J. Opt. Soc. Am.*, 1985, **2**, pp. 1160–1169
27 Adini, Y., Moses, Y., Ullman, S.: 'Face recognition: the problem of compensation for changes in illumination direction', *IEEE Trans. Pattern Anal. Mach. Intell.*, 1997, **19**, pp. 721–732
28 Shashua, A., Riklin-Raviv, T.: 'The quotient image: class-based re-rendering and recognition with varying illuminations', *IEEE Trans. Pattern Anal. Mach. Intell.*, 2001, **23**, pp. 129–139
29 Garcia, C., Zikos, G., Tziritas, G.: 'A wavelet-based framework for face recognition'. Proc. Workshop on Advances in Facial Image Analysis and Recognition Technology, 5th European Conf. On Computer Vision (ECCV '98), Freiburg Allemagne, pp. 84–92
30 Jobson, D., Rahman, Z., Woodell, G.: 'A multiscale retinex for bridging the gap between color images and the human observation of scenes', *IEEE Trans. Image Process.*, 1997, **6**, pp. 965–976
31 Gross, R., Brajovic, V.: 'An image preprocessing algorithm for illumination invariant face recognition', *Audio Video Based Biometric Person Authentication*, 2003, **2688**, pp. 10–18
32 Land, E.: 'An alternative technique for the computation of the designator in the retinex theory of color vision', *Proc. Nat. Acad. Sci.*, 1986, **83**, pp. 3078–3080
33 Horn, B.: 'Computer vision' (MIT Press, Cambridge, Mass, 1986)
34 Wang, L., Wang, X., Zhang, X., *et al*..: 'The equivalence of two dimensional PCA to line-based PCA', *Pattern Recognit. Lett.*, 2005, **1**, pp. 57–60
35 Ming, L., Yuan, B.: '2-D-LDA: a statistical linear discriminant analysis for image matrix', *Pattern Recognit. Lett.*, 2005, **26**, pp. 527–532
36 Sanayha, W., Rangsanseri, Y.: 'Relevance weighted $(2D)^2$LDA image projection technique for face recognition application'. Electrical Engineering/Electronics, Telecommunications and Information Technology, 2009, Sixth Int. Conf., vol. 2, pp. 663–667
37 Yale University Face Database: http://www.cvc.yale.edu/projects/yalefaces/yalefaces.html
38 ORL Face Database: http://www.cl.cam.ac.uk/Research/DTG/attarchive:pub/data/att_faces.zip
39 CAS-PEAL Face Database: http://www.jdl.ac.cn/peal/index.html
40 CMU PIE Face Database: http://www.ri.cmu.edu/projects/project_418.html

doi: 10.1049/iet-ipr.2013.0006